The Journal of Chemical Physics

Accurate prediction and measurement of vibronic branching ratios for laser cooling linear polyatomic molecules

Cite as: J. Chem. Phys. **155**, 091101 (2021); https://doi.org/10.1063/5.0063611
Submitted: 15 July 2021 • Accepted: 19 August 2021 • Published Online: 03 September 2021

Chaoqun Zhang, Benjamin L. Augenbraun, Zack D. Lasner, et al.

AIP Publishing

The Journal of Chemical Physics COMMUNICATION scitation.org/journal/jcp

Accurate prediction and measurement of vibronic branching ratios for laser cooling linear polyatomic molecules

Cite as: J. Chem. Phys. 155, 091101 (2021); doi: 10.1063/5.0063611
Submitted: 15 July 2021 • Accepted: 19 August 2021 •
Published Online: 3 September 2021

Chaoqun Zhang,[1] Benjamin L. Augenbraun,[2,3,a)] Zack D. Lasner,[2,3] Nathaniel B. Vilas,[2,3] John M. Doyle,[2,3] and Lan Cheng[1,b)]

AFFILIATIONS

[1] Department of Chemistry, The Johns Hopkins University, Baltimore, Maryland 21218, USA
[2] Department of Physics, Harvard University, Cambridge, Massachusetts 02138, USA
[3] Harvard-MIT Center for Ultracold Atoms, Cambridge, Massachusetts 02138, USA

[a)] **Electronic mail:** augenbraun@g.harvard.edu
[b)] **Author to whom correspondence should be addressed:** lcheng24@jhu.edu

ABSTRACT

We report a generally applicable computational and experimental approach to determine vibronic branching ratios in linear polyatomic molecules to the 10^{-5} level, including for nominally symmetry-forbidden transitions. These methods are demonstrated in CaOH and YbOH, showing approximately two orders of magnitude improved sensitivity compared with the previous state of the art. Knowledge of branching ratios at this level is needed for the successful deep laser cooling of a broad range of molecular species.

INTRODUCTION

Recent years have seen rapid progress in producing cold molecules and in using them to study molecular interactions and reactions,[1–3] quantum information processing and computation,[4–10] and precision measurement in search of new physics beyond the standard model (BSM).[11–14] Direct laser cooling and trapping has emerged as a particularly promising approach[5,15–30] to make molecules ultracold, as required by much of the current and future research in these areas. While molecules, compared to atoms, have wider applicability and often have higher sensitivity for BSM searches, their complex internal motions continue to pose challenges to applying the most powerful laser cooling techniques. The use of magneto-optical traps (MOTs) and very high-fidelity optical readout of internal quantum states typically rely on scattering more than 10^4 photons;[15,16] to achieve this, a transition manifold with the overall fractional loss less than 10^{-4} is required.

Several diatomic molecules have been optically cycled well above the required 10^4 photon threshold, leading to successful laser cooling[17,18] and loading into optical traps.[20,23–26] Laser cooling of polyatomic molecules, however, is more challenging. To understand the difficulty, this key metric should be considered—the quasidiagonality of the Franck–Condon matrix for the electronic laser cooling transition.[31–36] In order to quantify this metric, and thus determine whether a molecular candidate can be successfully loaded and held in a MOT, knowledge of all decays with intensity above about 10^{-5} is needed to ensure that a sufficient number of photons may be scattered by each molecule. Recent observations of nominally symmetry-forbidden decays[37,38] confirm that very weak decays, which can only be observed with considerable effort, can pose major obstacles to achieving an optical cycle capable of scattering $>10^4$ photons per molecule. While experimental studies using high resolution laser spectroscopy[30,37,39–43] have the potential to provide accurate branching ratios, it is a formidable endeavor to measure branching ratios smaller than 10^{-3} with current methods. The capability to calculate and measure the vibrational branching ratios accurately is thus a critical tool for developing laser cooling strategies for specific molecules.

In this Communication, we present generally applicable methods to calculate and measure vibronic branching ratios for all transitions with intensity above 10^{-5} in laser-coolable linear

polyatomic molecules. Spin-vibronic perturbations[44–46] contribute significantly to vibronic decay pathways so that modeling their effects on laser cooling is of utmost importance. The present computational scheme performs coupled-cluster (CC)[47–50] calculations to parameterize a Köppel–Domcke–Cederbaum (KDC) multi-state quasidiabatic Hamiltonian[51] including all relevant spin-vibronic perturbations and obtains vibronic levels and wave functions from discrete variable representation (DVR)[52–54] calculations. We compare the computational results to new measurements of branching ratios in CaOH and YbOH, with ~10^{-5} relative intensity sensitivity. These measurements, which rely crucially on strong optical excitation, achieve a level of sensitivity with direct experimental access to the perturbations probed by our calculations. The good agreement between experiment and theory demonstrated here validates both methodologies for guiding the selection of candidate molecules for direct laser cooling and for understanding the role that weak perturbations play in the optical cycling process. It also provides clear pathways for deep laser cooling of the two studied species, for use in quantum computation and in the search of physics BSM. These methods, in general, provide an approach for assessing and understanding laser cooling of polyatomic molecules.

THEORY

As shown in Fig. 1, the most commonly used optical cycle in a linear triatomic molecule of the type M-A-B, e.g., a metal hydroxide, involves the transitions from $A^2\Pi_{1/2}(000)$, the vibrational ground state of a low-lying excited electronic state, to the vibrational states of the ground electronic state $X^2\Sigma_{1/2}$, i.e., $X^2\Sigma_{1/2}(000)$, $X^2\Sigma_{1/2}(100)$, $X^2\Sigma_{1/2}(010)$, etc. Here, $(v_1 v_2^{\ell} v_3)$ denotes a vibrational state with v_1 quanta of excitation in the M-A stretching mode, v_2 quanta of bending excitation, and v_3 quanta of A-B stretching excitation. The superscript ℓ denotes a vibrational angular momentum due to bending excitations. $X^2\Sigma_{1/2}$ is well separated from other electronic states. A variational vibrational calculation within the Born–Oppenheimer approximation thus can produce its vibrational levels and wave functions accurately.

In contrast, a number of small perturbations[44–46] contributes to the $A^2\Pi_{1/2}(000)$ vibronic wave function and hence to the targeted

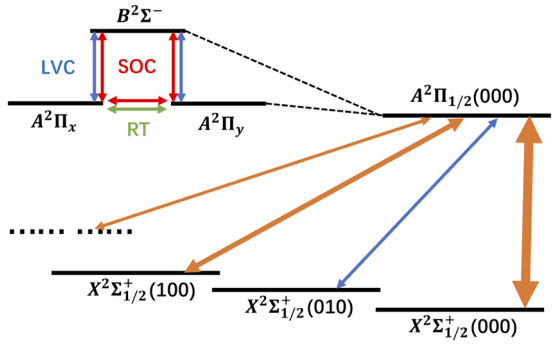

FIG. 1. Schematic illustration of small perturbations contributing to the $A^2\Pi_{1/2}(000)$ vibronic wavefunction as well as transitions to vibrational states of ground electronic states pertinent to laser cooling. SOC, LVC, and RT stand for spin–orbit coupling, linear vibronic coupling, and Renner–Teller coupling, respectively. The blue arrow denotes a nominally symmetry-forbidden transition.

branching ratios. The Renner–Teller (RT) effects[55] and spin–orbit coupling (SOC) are well known to play important roles in the description of vibronic levels and wave functions for the $A^2\Pi$ states in a linear triatomic molecule.[56,57] In addition, importantly, linear vibronic coupling (LVC) and SOC between $A^2\Pi$ and $B^2\Sigma$ introduce $A^2\Pi(010)$ and $B^2\Sigma(010)$ components into the wave function of $A^2\Pi_{1/2}(000)$ and thus make important contributions to nominally symmetry-forbidden transitions to $X^2\Sigma_{1/2}(010)$[58,59] with small but non-negligible branching factors. Therefore, aiming to obtain accurate branching factors higher than 10^{-5}, it is necessary to calculate the $A^2\Pi_{1/2}(000)$ vibronic wave function using a multi-state Hamiltonian with all of these relevant perturbations taken into account. We thus adopt the KDC Hamiltonian widely used to account for spin–vibronic coupling in spectrum simulation.[60–70] We mention that LVC between $A^2\Pi$ and $B^2\Sigma$ borrows intensity for the $B^2\Sigma(000) \rightarrow X^2\Sigma(010)$ transition in a similar way and thus will be relevant when studying the $B^2\Sigma \rightarrow X^2\Sigma$ cycling.

We use a KDC Hamiltonian of a form

$$\begin{bmatrix} E^{\rm qd}_{A^2\Pi_x} & V^{\rm RT}_{\rm xy} + ih^{\rm SO}_{\rm AA} & V^{\rm LVC}_{\rm xB} & 0 & 0 & h^{\rm SO}_{\rm AB} \\ V^{\rm RT}_{\rm yx} - ih^{\rm SO}_{\rm AA} & E^{\rm qd}_{A^2\Pi_y} & V^{\rm LVC}_{\rm yB} & 0 & 0 & ih^{\rm SO}_{\rm AB} \\ V^{\rm LVC}_{\rm Bx} & V^{\rm LVC}_{\rm By} & E^{\rm qd}_{B^2\Sigma} & -h^{\rm SO}_{\rm BA} & -ih^{\rm SO}_{\rm BA} & 0 \\ 0 & 0 & -h^{\rm SO}_{\rm AB} & E^{\rm qd}_{A^2\Pi_x} & V^{\rm RT}_{\rm xy} - ih^{\rm SO}_{\rm AA} & V^{\rm LVC}_{\rm xB} \\ 0 & 0 & ih^{\rm SO}_{\rm AB} & V^{\rm RT}_{\rm yx} + ih^{\rm SO}_{\rm AA} & E^{\rm qd}_{A^2\Pi_y} & V^{\rm LVC}_{\rm yB} \\ h^{\rm SO}_{\rm BA} & -ih^{\rm SO}_{\rm BA} & 0 & V^{\rm LVC}_{\rm Bx} & V^{\rm LVC}_{\rm By} & E^{\rm qd}_{B^2\Sigma} \end{bmatrix} \tag{1}$$

including six-scalar quasidiabatic electronic states, $A^2\Pi_x(\alpha)$, $A^2\Pi_y(\alpha)$, $B^2\Sigma(\alpha)$, $A^2\Pi_x(\beta)$, $A^2\Pi_y(\beta)$, and $B^2\Sigma(\beta)$, as the electronic basis. Here, α and β refer to $S_z = 1/2$ and $-1/2$. $E^{\rm qd}_{A^2\Pi_x}$, $E^{\rm qd}_{A^2\Pi_y}$, and $E^{\rm qd}_{B^2\Sigma}$ denote potential energies of these quasidiabatic states. $V^{\rm RT}$'s represent RT coupling, $V^{\rm LVC}$'s represent LVC, and $h^{\rm SO}$'s denote SOC matrix elements. This Hamiltonian includes all the perturbations pertinent to the calculations of branching ratios for the $A^2\Pi_{1/2} \rightarrow X^2\Sigma_{1/2}$ optical cycle.

We first calculate the adiabatic potential energy surfaces (PESs) for $A^2\Pi_+$ and $A^2\Pi_-$, the two scalar adiabatic states of $A^2\Pi$, as well as for $B^2\Sigma$,

$$\begin{bmatrix} E^{\rm ad}_{A^2\Pi_+} & 0 & 0 \\ 0 & E^{\rm ad}_{A^2\Pi_-} & 0 \\ 0 & 0 & E^{\rm ad}_{B^2\Sigma} \end{bmatrix}. \tag{2}$$

Then, we apply the following adiabatic to diabatic transformation:

$$\begin{bmatrix} \dfrac{Q_x}{\sqrt{Q_x^2+Q_y^2}} & \dfrac{Q_y}{\sqrt{Q_x^2+Q_y^2}} \\ \dfrac{Q_y}{\sqrt{Q_x^2+Q_y^2}} & -\dfrac{Q_x}{\sqrt{Q_x^2+Q_y^2}} \end{bmatrix}, \tag{3}$$

where Q_x and Q_y represent the normal coordinates of the two bending modes. This transformation was derived for harmonic potentials. The application to potentials with anharmonic contributions

corresponds to a quasidiabatization process. This transforms $A^2\Pi_+$ and $A^2\Pi_-$ into two quasidiabatic states, hereafter referred to as $A^2\Pi_x$ and $A^2\Pi_y$, and the adiabatic potentials in Eq. (2) into the quasidiabatic potentials

$$\begin{bmatrix} \widetilde{E}^{\mathrm{qd}}_{A^2\Pi_x} & \widetilde{V}^{\mathrm{RT}}_{\mathrm{xy}} & 0 \\ \widetilde{V}^{\mathrm{RT}}_{\mathrm{xy}} & \widetilde{E}^{\mathrm{qd}}_{A^2\Pi_y} & 0 \\ 0 & 0 & E^{\mathrm{ad}}_{B^2\Sigma} \end{bmatrix}. \tag{4}$$

Next, we include LVC using the linear diabatic coupling constants[71] between $A^2\Pi_{x(y)}$ and $B^2\Sigma$. This also introduces corrections to $\widetilde{E}^{\mathrm{qd}}$, $\widetilde{V}^{\mathrm{RT}}$, and $E^{\mathrm{ad}}_{B^2\Sigma}$,[71] leading to

$$\begin{bmatrix} E^{\mathrm{qd}}_{A^2\Pi_x} & V^{\mathrm{RT}}_{\mathrm{xy}} & V^{\mathrm{LVC}}_{\mathrm{xB}} \\ V^{\mathrm{RT}}_{\mathrm{xy}} & E^{\mathrm{qd}}_{A^2\Pi_y} & V^{\mathrm{LVC}}_{\mathrm{yB}} \\ V^{\mathrm{LVC}}_{\mathrm{Bx}} & V^{\mathrm{LVC}}_{\mathrm{By}} & E^{\mathrm{qd}}_{B^2\Sigma} \end{bmatrix}. \tag{5}$$

Finally, we augment Eq. (5) with SOC and obtain Eq. (1), hereby completing the construction of the quasidiabatic Hamiltonian.

We used the CFOUR program[49,72–75] to calculate all parameters in the KDC Hamiltonian including the adiabatic PESs, linear diabatic coupling constants,[71] and SOC matrix elements.[76–78] The present study used the equation-of-motion (EOM) electron attachment CC singles and doubles (EOMEA-CCSD) method[79] and correlation-consistent basis sets[80–84] to provide accurate PESs around the equilibrium structures pertinent to the calculations of the low-lying vibronic states involved in laser cooling. We accounted for scalar-relativistic effects for SrOH and YbOH using the spin-free exact two-component theory in its one-electron variant (SFX2C-1e).[85,86] Having the quasidiabatic Hamiltonians expanded in "real space" basis sets, we carried out DVR[53] calculations in the representation of the four vibrational normal coordinates to obtain vibronic levels and wave functions. The normal coordinate DVR calculations previously produced accurate vibrational levels for the $X^2\Sigma$ state of YbOH.[43] We then combine the Franck–Condon overlap integrals with the EOMEA-CCSD electronic transition dipole moments to obtain the branching factors. We refer the readers to the supplementary material for more details about the computations.

EXPERIMENT

Branching ratios for CaOH and YbOH were recorded using dispersed laser-induced fluorescence (DLIF) measurements. The sensitivity achieved was improved by approximately two orders of magnitude over previous measurements in similar species,[41–43,92] primarily due to the use of bright cryogenic molecular beams and photon cycling described below and in the supplementary material.

In brief, cryogenic buffer gas beams of CaOH and YbOH were produced using the beam source described in Ref. 14. Laser-excitation-enhanced chemical reactions between metallic Yb or Ca and H_2O vapor[93–95] increased the molecular beam flux by a factor of ~10 compared to previous reports.[14,27] The apparatus was modified with a spectrometer similar to that used in Ref. 38. After propagating ~30 cm downstream from the source, the molecules interacted with laser beams addressing the rotationally resolved $\tilde{A}\,^2\Pi_{1/2}(000) \leftarrow \tilde{X}\,^2\Sigma^+(000)$ and $\tilde{A}\,^2\Pi_{1/2}(000) \leftarrow \tilde{X}\,^2\Sigma^+(100)$ transitions used for optical cycling in laser cooling experiments.[14,27] In this detection region, each molecule scattered, on average, 50–100 photons. Using the optical cycling transitions therefore directly increased the number of photons collected and thus the sensitivity, compared to typical DLIF measurements where molecules scatter, on average, only a single photon.[41]

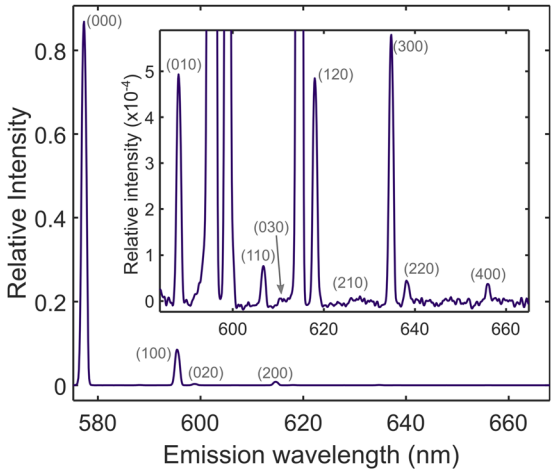

FIG. 2. Dispersed laser-induced fluorescence measurement following excitation of YbOH to the $\tilde{A}\,^2\Pi_{1/2}(000)$ $(J' = 1/2, p = +)$ state. Gray labels above each peak identify the ground state vibrational level (v_1, v_2, v_3) populated by that decay. Inset: additional detail near the noise floor, demonstrating that spectral features with relative intensities as low as about 2×10^{-5} can be identified.

The molecular fluorescence was collected and dispersed on a 0.67 m Czerny–Turner style spectrometer, before being detected with an electron-multiplying charged-coupled device (EMCCD). The wavelength and intensity axes were carefully calibrated in separate measurements (see the supplementary material). See the supplementary material for more details on the experimental apparatus, calibration, and data analysis. A representative DLIF spectrum recorded for YbOH is shown in Fig. 2, demonstrating the sensitivity achieved by this method.

RESULTS AND DISCUSSION

The computed vibronic energy levels for SrOH and CaOH, as summarized in Table I, show excellent agreement with measured values, with discrepancies lower than 10 cm^{-1}. The calculations also accurately reproduced the splittings between (02^20) and (02^00) and among the four $A^2\Pi(010)$ states. The present KDC Hamiltonian calculations thus accurately describe the vibronic wave functions. We provide a complete list of computed vibronic levels for the $X^2\Sigma$, $A^2\Pi$, and $B^2\Sigma$ states in the supplementary material.

Tables II and III summarize the calculated and measured vibrational branching ratios for decay from $A^2\Pi_{1/2}(000)$ to the $X^2\Sigma$ state in CaOH and YbOH. All branching ratios above 10^{-5} are shown; computed branching to the O–H stretch mode is below 10^{-6} and therefore negligible. The present level of consistency between computations and measurements for CaOH and YbOH, i.e., excellent agreement for stronger transitions and qualitative agreement for weaker transitions below 0.1%, is very promising. In CaOH,

TABLE I. Relative vibrational energy levels (in cm^{-1}) of the $X^2\Sigma_{1/2}$ and $A^2\Pi_{1/2}$ states in CaOH and SrOH.

	CaOH		SrOH	
State	Calculated	Expt.[a]	Calculated	Expt.[42,87]
$X^2\Sigma_{1/2}(000)$	0	0.0	0	0.0
$X^2\Sigma_{1/2}(010)$	355	352.9	367	363.7
$X^2\Sigma_{1/2}(100)$	611	609.0	534	527.0
$X^2\Sigma_{1/2}(02^00)$	695	688.7	702	703.3
$X^2\Sigma_{1/2}(02^20)$	718	713.0	736	733.5
$X^2\Sigma_{1/2}(110)$	954	952	892	⋯
$X^2\Sigma_{1/2}(200)$	1214	1210.2	1063	1049.1
$A^2\Pi_{1/2}(000)$	0	0.0	0	0.0
$A^2\Pi_{3/2}(000)$	67	66.8	254	263.5
$A^2\Pi_{1/2}(010)$	346	345	379	377.8
$A^2\Pi_{1/2}(010)$	362	360	383	380.4
$A^2\Pi_{1/2}(100)$	623	628.7	552	542.1
$A^2\Pi_{3/2}(010)$	428	425	636	641.8
$A^2\Pi_{3/2}(010)$	446	445	642	648.4
$A^2\Pi_{3/2}(100)$	690	695.9	808	806.6

[a]Levels for the $X^2\Sigma$ states from Refs. 88–90. Levels for the $A^2\Pi$ states from Refs. 59, 89, and 91. $A^2\Pi(010)$ levels taken as $J = 0$ results in Fig. 3 of Ref. 89.

TABLE III. The vibrational level positions (in cm^{-1}) of the $X^2\Sigma$ state of YbOH and vibrational branching ratios (VBRs) of the transitions from $A^2\Pi_{1/2}(000)$ to these states. The measured vibrational frequencies have an estimated uncertainty of ±5 cm^{-1}, and the noise level of the smallest branching ratios is at the level of 9×10^{-6}. Anharmonic splittings in the (020) and (120) levels were not resolved.

	Level		VBR	
State	Calculated	Experiment	Calculated (%)	Experiment (%)
(000)	0	0	87.691	89.44(61)
(010)	322	319	0.053	0.054(4)
(100)	532	528	10.774	9.11(55)
(02^00)	631	627	0.457	0.335(20)
(02^20)	654	⋯	0.022	⋯
(110)	846	840	0.007	0.0100(13)
(03^10)	952	947	<0.001	0.0020(9)
(200)	1062	1052	0.863	0.914(62)
(12^00)	1154	1144	0.063	0.055(4)
(12^20)	1173	⋯	0.004	⋯
(210)	1369	1369	<0.001	0.0019(12)
(300)	1600	1572	0.054	0.067(4)
(22^00)	1680	1651	0.007	0.0050(9)
(400)	2160	2079	0.002	0.0045(9)

although branching ratios for the origin transitions are as large as ~95%, one has to take into account up to (300) to saturate the Ca–O stretch branching ratios to below 10^{-5}. In YbOH, the branching ratios for the Yb–O stretch are less diagonal and (400) is relevant.

The nominally symmetry-forbidden $|\Delta v_2| = 1, 3, 5, \ldots$ transitions borrow intensities through vibronic and/or spin–orbit coupling.[37,58,59] As shown in Fig. 3, the "direct vibronic coupling" (DVC) mechanism mixes $B^2\Sigma(010)$ into the $A^2\Pi_{1/2}(000)$ wave function through LVC. The "spin–orbit-vibronic coupling" (SOVC) mechanism couples $B^2\Sigma(000)$ with $A^2\Pi(000)$ through SOC and then mixes $A^2\Pi_{3/2}(010)$ into the $A^2\Pi_{1/2}(000)$ wave function through LVC. A perturbative analysis gives the following ratio between the SOVC and DVC contributions to the intensity:

$$\frac{I_{\mathrm{SOVC}}}{I_{\mathrm{DVC}}} = 2\frac{|h_{\mathrm{BA}}^{\mathrm{SO}}|^2|h_{\mathrm{AX}}^{\mathrm{dip}}|^2}{|\omega(010) + 2h_{\mathrm{AA}}^{\mathrm{SO}}|^2|h_{\mathrm{BX}}^{\mathrm{dip}}|^2}, \tag{6}$$

TABLE II. Branching ratios for transitions from $A^2\Pi_{1/2}(000)$ to vibrational levels of $X^2\Sigma_{1/2}$ in CaOH and SrOH. The noise level of the smallest branching ratios for CaOH is at the level of 7×10^{-6}; the uncertainty in the larger branching ratios is dominated by spectrometer calibration. The relative intensities of the unresolved $\ell = 0, 2$ components of the (020) and (120) manifolds were fixed to the value measured in previous work.[37]

	CaOH		SrOH	
State	Calculated (%)	Experiment (%)	Calculated (%)	Experiment (%)[42]
(000)	95.429	94.59(29)	94.509	95.7
(010)	0.063	0.099(6)	0.025	⋯
(100)	3.934	4.75(27)	5.188	4.3
(02^00)	0.298	0.270(17)	0.010	⋯
(02^20)	0.079	0.067(12)	0.036	⋯
(110)	0.003	0.0064(7)	0.001	⋯
(03^10)	<0.001	0.0034(8)	<0.001	⋯
(200)	0.157	0.174(16)	0.218	⋯
(12^00)	0.022	0.021(3)	<0.001	⋯
(12^20)	0.005	0.005(1)	0.003	⋯
(040)	<0.001	0.0021(7)	<0.001	⋯
(300)	0.006	0.0068(8)	0.008	⋯
(22^00)	0.002	0.0020(7)	<0.001	⋯

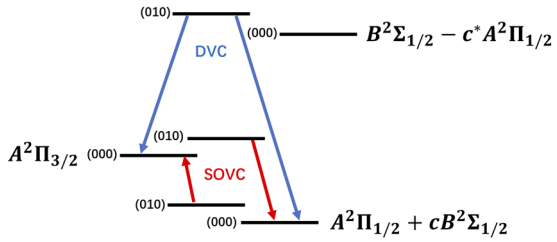

FIG. 3. The direct vibronic coupling (DVC) and spin–orbit–vibronic coupling (SOVC) mechanisms for borrowing intensities for the nominally symmetry-forbidden $A^2\Pi(000) \rightarrow X^2\Sigma(010)$ transition. $c = \sqrt{2}\frac{h_{BA}^{SO}}{E_A - E_B}$ accounts for the SO mixing of A and B states.

where h_{AX}^{dip} and h_{BX}^{dip} are the A-X and B-X electronic transition dipole moments. The percentages of the DVC contributions obtained using the $B^2\Sigma(010)$ and $A^2\Pi(010)$ components in the computed $A^2\Pi_{1/2}(000)$ wave function amount to 98%, 89%, and 70% for CaOH, SrOH, and YbOH, respectively, which are consistent with the values of 99%, 92%, and 76% obtained from the perturbative analysis using Eq. (6). The DVC channel dominates this intensity borrowing process even in molecules containing heavy atoms since the effects of large h_{BA}^{SO} are offset by large h_{AA}^{SO} in the denominator.

It is desirable to minimize the coupling between $X^2\Sigma(100)$ and $X^2\Sigma(020)$ in designing laser-coolable linear triatomic molecules. As shown in Table II, the intensities of the transitions to $X^2\Sigma(020)$ in SrOH are significantly lower than in CaOH. This is due to the larger energy separation between the $X^2\Sigma(100)$ and $X^2\Sigma(020)$ levels in SrOH (534 and 702 cm^{-1}) compared to CaOH (611 and 694 cm^{-1}), and hence weaker coupling. Similarly, there is non-negligible vibrational branching to $X^2\Sigma(120)$ and $X^2\Sigma(220)$ of CaOH; in contrast, the branching ratio to $X^2\Sigma(120)$ in SrOH is lower than 10^{-6}.

CONCLUSION

We have presented a computational and experimental scheme to determine vibronic branching ratios pertinent to scattering around 100 000 photons in linear polyatomic molecules. The computational methodology is generally applicable to the study of optical cycles for linear triatomic molecules, such as metal hydroxides and isocyanides proposed for laser cooling. We have found good agreement with new experimental measurements that used optical cycling to achieve relative intensity sensitivities at the 10^{-5} level. The agreement supports the accuracy of both theoretical and experimental techniques.

Further work for the future includes the study of the accuracy for the parameterization of the quasidiabatic Hamiltonian, including the higher-order correlation effects on PESs, the effects of quadratic vibronic coupling, and rovibrational coupling, aiming to obtain quantitative accuracy for weak transitions. It is also of interest to study the transitions involving dark electronic states[26,28,96,97] in linear triatomic molecules, such as BaOH. The generalization to calculations of linear tetraatomic molecules, e.g., metal monoacetylides, should also provide very interesting results. The calculation of nonlinear molecules is the next frontier, and we assess that we can follow the same generic scheme although the perturbations relevant to the calculations will be molecule specific. The computational framework presented here thus forms a basis for the calculation of vibronic levels and branching ratios that are sufficiently accurate and complete to facilitate and guide laser cooling experiments for even highly complex polyatomic molecules.

SUPPLEMENTARY MATERIAL

The supplementary material contains details of experimental measurements and computations for the sake of self-containedness and a complete account of computed vibronic levels.

ACKNOWLEDGMENTS

C.Z. thanks Yifan Shen (Baltimore) for stimulating discussions. L.C. is grateful to Paul Dagdigian (Baltimore) and John Stanton (Gainesville) for reading the manuscript and for helpful comments. This computational work at the Johns Hopkins University was supported by the National Science Foundation, under Grant No. PHY-2011794. All calculations were carried out at the Maryland Advanced Research Computing Center (MARCC). CaOH measurements were supported by the AFOSR and NSF. YbOH measurements were supported by the Heising-Simons Foundation, the Gordon and Betty Moore Foundation, and the Alfred P. Sloan Foundation. N.B.V. acknowledges support from the NDSEG fellowship.

DATA AVAILABILITY

The data that support the findings of this study are available within this article and its supplementary material.

REFERENCES

[1] S. Ospelkaus, K.-K. Ni, D. Wang, M. H. G. de Miranda, B. Neyenhuis, G. Quéméner, P. S. Julienne, J. L. Bohn, D. S. Jin, and J. Ye, Science **327**, 853 (2010).
[2] G. Quéméner and P. S. Julienne, Chem. Rev. **112**, 4949 (2012).
[3] J. L. Bohn, A. M. Rey, and J. Ye, Science **357**, 1002 (2017).
[4] D. DeMille, Phys. Rev. Lett. **88**, 067901 (2002).
[5] L. D. Carr, D. DeMille, R. V. Krems, and J. Ye, New J. Phys. **11**, 055049 (2009).
[6] Q. Wei, S. Kais, B. Friedrich, and D. Herschbach, J. Chem. Phys. **135**, 154102 (2011).
[7] M. Karra, K. Sharma, B. Friedrich, S. Kais, and D. Herschbach, J. Chem. Phys. **144**, 094301 (2016).
[8] E. R. Hudson and W. C. Campbell, Phys. Rev. A **98**, 040302 (2018).
[9] K.-K. Ni, T. Rosenband, and D. D. Grimes, Chem. Sci. **9**, 6830 (2018).
[10] P. Yu, L. W. Cheuk, I. Kozyryev, and J. M. Doyle, New J. Phys. **21**, 093049 (2019).
[11] T. Zelevinsky, S. Kotochigova, and J. Ye, Phys. Rev. Lett. **100**, 043201 (2008).
[12] I. Kozyryev and N. R. Hutzler, Phys. Rev. Lett. **119**, 133002 (2017).
[13] J. Lim, J. R. Almond, M. A. Trigatzis, J. A. Devlin, N. J. Fitch, B. E. Sauer, M. R. Tarbutt, and E. A. Hinds, Phys. Rev. Lett. **120**, 123201 (2018).
[14] B. L. Augenbraun, Z. D. Lasner, A. Frenett, H. Sawaoka, C. Miller, T. C. Steimle, and J. M. Doyle, New J. Phys. **22**, 022003 (2020).
[15] M. Di Rosa, Eur. Phys. J. D **31**, 395 (2004).
[16] B. K. Stuhl, B. C. Sawyer, D. Wang, and J. Ye, Phys. Rev. Lett. **101**, 243002 (2008).
[17] E. S. Shuman, J. F. Barry, and D. DeMille, Nature **467**, 820 (2010).

[18]M. T. Hummon, M. Yeo, B. K. Stuhl, A. L. Collopy, Y. Xia, and J. Ye, Phys. Rev. Lett. **110**, 143001 (2013).
[19]V. Zhelyazkova, A. Cournol, T. E. Wall, A. Matsushima, J. J. Hudson, E. Hinds, M. Tarbutt, and B. Sauer, Phys. Rev. A **89**, 053416 (2014).
[20]J. F. Barry, D. J. McCarron, E. B. Norrgard, M. H. Steinecker, and D. DeMille, Nature **512**, 286 (2014).
[21]I. Kozyryev, L. Baum, K. Matsuda, and J. M. Doyle, ChemPhysChem **17**, 3641 (2016).
[22]I. Kozyryev, L. Baum, K. Matsuda, B. L. Augenbraun, L. Anderegg, A. P. Sedlack, and J. M. Doyle, Phys. Rev. Lett. **118**, 173201 (2017).
[23]S. Truppe, H. J. Williams, M. Hambach, L. Caldwell, N. J. Fitch, E. A. Hinds, B. E. Sauer, and M. R. Tarbutt, Nat. Phys. **13**, 1173 (2017).
[24]L. Anderegg, B. L. Augenbraun, E. Chae, B. Hemmerling, N. R. Hutzler, A. Ravi, A. Collopy, J. Ye, W. Ketterle, and J. M. Doyle, Phys. Rev. Lett. **119**, 103201 (2017).
[25]H. J. Williams, L. Caldwell, N. J. Fitch, S. Truppe, J. Rodewald, E. A. Hinds, B. E. Sauer, and M. R. Tarbutt, Phys. Rev. Lett. **120**, 163201 (2018).
[26]A. L. Collopy, S. Ding, Y. Wu, I. A. Finneran, L. Anderegg, B. L. Augenbraun, J. M. Doyle, and J. Ye, Phys. Rev. Lett. **121**, 213201 (2018).
[27]L. Baum, N. B. Vilas, C. Hallas, B. L. Augenbraun, S. Raval, D. Mitra, and J. M. Doyle, Phys. Rev. Lett. **124**, 133201 (2020).
[28]S. Ding, Y. Wu, I. A. Finneran, J. J. Burau, and J. Ye, Phys. Rev. X **10**, 021049 (2020).
[29]D. Mitra, N. B. Vilas, C. Hallas, L. Anderegg, B. L. Augenbraun, L. Baum, C. Miller, S. Raval, and J. M. Doyle, Science **369**, 1366 (2020).
[30]B. L. Augenbraun, J. M. Doyle, T. Zelevinsky, and I. Kozyryev, Phys. Rev. X **10**, 031022 (2020).
[31]T. A. Isaev and R. Berger, Phys. Rev. Lett. **116**, 063006 (2016); arXiv:1504.08326.
[32]M. Li, J. Kłos, A. Petrov, and S. Kotochigova, Commun. Phys. **2**, 148 (2019); arXiv:1904.11579.
[33]Y. Hao, L. F. Pašteka, L. Visscher, P. Aggarwal, H. L. Bethlem, A. Boeschoten, A. Borschevsky, M. Denis, K. Esajas, S. Hoekstra, K. Jungmann, V. R. Marshall, T. B. Meijknecht, M. C. Mooij, R. G. E. Timmermans, A. Touwen, W. Ubachs, L. Willmann, Y. Yin, and A. Zapara, J. Chem. Phys. **151**, 034302 (2019).
[34]M. V. Ivanov, F. H. Bangerter, and A. I. Krylov, Phys. Chem. Chem. Phys. **21**, 19447 (2019).
[35]M. V. Ivanov, T.-C. Jagau, G.-Z. Zhu, E. R. Hudson, and A. I. Krylov, Phys. Chem. Chem. Phys. **22**, 17075 (2020).
[36]C. E. Dickerson, H. Guo, A. J. Shin, B. L. Augenbraun, J. R. Caram, W. C. Campbell, and A. N. Alexandrova, Phys. Rev. Lett. **126**, 123002 (2021).
[37]L. Baum, N. B. Vilas, C. Hallas, B. L. Augenbraun, S. Raval, D. Mitra, and J. M. Doyle, Phys. Rev. A **103**, 043111 (2021).
[38]B. L. Augenbraun, Z. D. Lasner, A. Frenett, H. Sawaoka, A. T. Le, J. M. Doyle, and T. C. Steimle, Phys. Rev. A **103**, 022814 (2021).
[39]P. M. Sheridan, M. J. Dick, J.-G. Wang, and P. F. Bernath, Mol. Phys. **105**, 569 (2007).
[40]S. Nakhate, T. C. Steimle, N. H. Pilgram, and N. R. Hutzler, Chem. Phys. Lett. **715**, 105 (2019).
[41]I. Kozyryev, T. C. Steimle, P. Yu, D. T. Nguyen, and J. M. Doyle, New J. Phys. **21**, 052002 (2019); arXiv:1812.05636.
[42]D.-T. Nguyen, T. C. Steimle, I. Kozyryev, M. Huang, and A. B. McCoy, J. Mol. Spectrosc. **347**, 7 (2018).
[43]E. T. Mengesha, A. T. Le, T. C. Steimle, L. Cheng, C. Zhang, B. L. Augenbraun, Z. Lasner, and J. Doyle, J. Phys. Chem. A **124**, 3135 (2020).
[44]H. Lefebvre-Brion and R. W. Field, *The Spectra and Dynamics of Diatomic Molecules* (Elsevier, New York, 2004).
[45]P. F. Bernath, *Spectra of Atoms and Molecules* (Oxford University Press, 2020).
[46]E. Hirota, *High-Resolution Spectroscopy of Transient Molecules* (Springer-Verlag, Berlin, 1985).
[47]T. D. Crawford and H. F. Schaefer III, Rev. Comput. Chem. **14**, 33 (2000).
[48]R. J. Bartlett and M. Musiał, Rev. Mod. Phys. **79**, 291 (2007).
[49]J. F. Stanton and R. J. Bartlett, J. Chem. Phys. **98**, 7029 (1993).
[50]A. I. Krylov, Annu. Rev. Phys. Chem. **59**, 433 (2008).
[51]H. Köppel, W. Domcke, and L. S. Cederbaum, Adv. Chem. Phys. **57**, 59 (1984).
[52]J. C. Light, I. P. Hamilton, and J. V. Lill, J. Chem. Phys. **82**, 1400 (1985).
[53]D. T. Colbert and W. H. Miller, J. Chem. Phys. **96**, 1982 (1992).
[54]J. C. Light and T. Carrington, Jr., Adv. Chem. Phys. **114**, 263 (2000).
[55]R. Renner, Z. Phys. **92**, 172 (1934).
[56]S. Carter and N. C. Handy, Mol. Phys. **52**, 1367 (1984).
[57]S. Carter, N. C. Handy, P. Rosmus, and G. Chambaud, Mol. Phys. **71**, 605 (1990).
[58]C. R. Brazier and P. F. Bernath, J. Mol. Spectrosc. **114**, 163 (1985).
[59]J. A. Coxon, M. G. Li, and P. I. Presunka, J. Mol. Spectrosc. **164**, 118 (1994).
[60]H. Köppel, W. Domcke, and L. S. Cederbaum, J. Chem. Phys. **74**, 2945 (1981).
[61]J. Schmidt-Klügmann, H. Köppel, S. Schmatz, and P. Botschwina, Chem. Phys. Lett. **369**, 21 (2003).
[62]A. V. Marenich and J. E. Boggs, J. Chem. Phys. **122**, 024308 (2004).
[63]S. Mishra, W. Domcke, and L. V. Poluyanov, Chem. Phys. **327**, 457 (2006).
[64]S. Mishra, L. V. Poluyanov, and W. Domcke, J. Chem. Phys. **126**, 134312 (2007).
[65]M. S. Schuurman, D. E. Weinberg, and D. R. Yarkony, J. Chem. Phys. **127**, 104309 (2007).
[66]E. Garand, K. Klein, J. F. Stanton, J. Zhou, T. I. Yacovitch, and D. M. Neumark, J. Phys. Chem. A **114**, 1374 (2010).
[67]J. Nagesh and E. L. Sibert, J. Phys. Chem. A **116**, 3846 (2012).
[68]Z. Shao and Y. Mo, J. Chem. Phys. **138**, 244309 (2013).
[69]M. Weichman, L. Cheng, J. B. Kim, J. F. Stanton, and D. M. Neumark, J. Chem. Phys. **146**, 224309 (2017).
[70]S. Scheit, S. Goswami, H.-D. Meyer, and H. Köppel, Comput. Theor. Chem. **1150**, 71 (2019).
[71]T. Ichino, J. Gauss, and J. F. Stanton, J. Chem. Phys. **130**, 174105 (2009).
[72]J. F. Stanton, J. Gauss, L. Cheng, M. E. Harding, D. A. Matthews, and P. G. Szalay, CFOUR, Coupled-Cluster techniques for Computational Chemistry, a quantum-chemical program package, with contributions from A. A. Auer, R. J. Bartlett, U. Benedikt, C. Berger, D. E. Bernholdt, Y. J. Bomble, O. Christiansen, F. Engel, R. Faber, M. Heckert, O. Heun, M. Hilgenberg, C. Huber, T.-C. Jagau, D. Jonsson, J. Jusélius, T. Kirsch, K. Klein, W. J. Lauderdale, F. Lipparini, T. Metzroth, L. A. Mück, D. P. O'Neill, D. R. Price, E. Prochnow, C. Puzzarini, K. Ruud, F. Schiffmann, W. Schwalbach, C. Simmons, S. Stopkowicz, A. Tajti, J. Vázquez, F. Wang, and J. D. Watts and the integral packages MOLECULE (J. Almlöf and P. R. Taylor), PROPS (P. R. Taylor), ABACUS (T. Helgaker, H. J. Aa. Jensen, P. Jørgensen, and J. Olsen), and ECP routines by A. V. Mitin and C. van Wüllen, for the current version, see http://www.cfour.de.
[73]D. A. Matthews, L. Cheng, M. E. Harding, F. Lipparini, S. Stopkowicz, T.-C. Jagau, P. G. Szalay, J. Gauss, and J. F. Stanton, J. Chem. Phys. **152**, 214108 (2020).
[74]J. F. Stanton and J. Gauss, J. Chem. Phys. **111**, 8785 (1999).
[75]L. Cheng and J. Gauss, J. Chem. Phys. **135**, 084114 (2011).
[76]K. Klein and J. Gauss, J. Chem. Phys. **129**, 194106 (2008).
[77]L. Cheng, F. Wang, J. F. Stanton, and J. Gauss, J. Chem. Phys. **148**, 044108 (2018).
[78]C. Zhang and L. Cheng, Mol. Phys. **118**, e1768313 (2020).
[79]M. Nooijen and R. J. Bartlett, J. Chem. Phys. **102**, 3629 (1995).
[80]T. H. Dunning, Jr., J. Chem. Phys. **90**, 1007 (1989).
[81]J. Koput and K. A. Peterson, J. Phys. Chem. A **106**, 9595 (2002).
[82]W. A. De Jong, R. J. Harrison, and D. A. Dixon, J. Chem. Phys. **114**, 48 (2001).
[83]J. G. Hill and K. A. Peterson, J. Chem. Phys. **147**, 244106 (2017).
[84]Q. Lu and K. A. Peterson, J. Chem. Phys. **145**, 054111 (2016).
[85]K. G. Dyall, J. Chem. Phys. **115**, 9136 (2001).
[86]W. Liu and D. Peng, J. Chem. Phys. **131**, 031104 (2009).
[87]P. I. Presunka and J. A. Coxon, Chem. Phys. **190**, 97 (1995).
[88]J. A. Coxon, M. Li, and P. I. Presunka, Mol. Phys. **76**, 1463 (1992).
[89]M. Li and J. A. Coxon, J. Chem. Phys. **102**, 2663 (1995).
[90]R. Pereira and D. H. Levy, J. Chem. Phys. **105**, 9733 (1996).
[91]M. Li and J. A. Coxon, J. Chem. Phys. **104**, 4961 (1996).
[92]A. C. Paul, K. Sharma, M. A. Reza, H. Telfah, T. A. Miller, and J. Liu, J. Chem. Phys. **151**, 134303 (2019).
[93]W. T. M. L. Fernando, R. S. Ram, L. C. O'Brien, and P. F. Bernath, J. Phys. Chem. **95**, 2665 (1991).

[94]A. M. R. P. Bopegedera, C. R. Brazier, and P. F. Bernath, J. Phys. Chem. **91**, 2779 (1987).
[95]A. Jadbabaie, N. H. Pilgram, J. Klos, S. Kotochigova, and N. R. Hutzler, New J. Phys. **22**, 022002 (2020).
[96]A. L. Collopy, M. T. Hummon, M. Yeo, B. Yan, and J. Ye, New J. Phys. **17**, 055008 (2015).
[97]C. Zhang, H. Korslund, Y. Wu, S. Ding, and L. Cheng, Phys. Chem. Chem. Phys. **22**, 26167 (2020).